A mathematical analysis and experimental testing of the plastron's role in weight support and how it assists biomimetic water strider robots traversing the air water interface

William Snyder
Ossining High School
Ossining, NY

Abstract:

Many attempts have been made to construct robots that mimic water striders ability to transit the surface of the water. Research thus far has had some success creating these robots; however, the robots still do not produce a sufficient amount of lift force and are unable to support sensors and equipment necessary for real world tasks. This study mimics the non-wetting air pocket (plastron) formed on actual water striders' legs in an effort to increase supportive force, and conducts an in-depth analysis of the plastron and its affect on lift force through modeling and experimental testing of lift forces. Using a mathematical model it was determined that the lift force produced by the plastron comes almost exclusively from buoyancy forces. It was also determined that the plastron must be nearly ten times the volume of a 1mm in diameter leg to double the lift force produced by the leg. When experimentally testing the lift force of textured and untextured samples our results supported the conclusions of our modeling. These results however, are not in agreement with other previous research which has shown that water strider legs with a plastron have a much higher supportive force than a similar leg with a high contact angle and no plastron.

William Snyder
Personal Section

I entered my high school's science research program as a sophomore with little more to go on than an interest in aquatic robotics and biomimetics, a science involving using nature as a model for engineering. From there, I began to read scientific articles on the subject. From these articles, I learned of many prominent researchers doing work in the field. Just a few months in I was ready to contact a promising researcher working at a local lab on a project I loved. Just a few days later I got an e-mail back, in part, "I'm sorry that you are having such a hard time getting into a lab for research. It's very challenging, as many of the labs working in this area are just maxed out with personnel at the moment. Sadly, this includes my own. I do hope that you find something, and I urge you to be persistent." For the rest of that year and through the summer I tried many other labs, as they progressively got farther away, some responded similarly, some didn't respond at all. I was reading papers and planning experiments for which I had no facilities to carry out.

I finally found a lab at the beginning of my Junior year. A stretch in distance and topic area from my original search criteria. This was the nano-robotics lab at Carnegie Mellon University. The project wasn't exactly what I was looking for, but as I read the papers I became more and more interested, and began to realize that it had many things in common with the project I had wanted to do in the first place. The project involved robots that walk on top of the water instead of below it and these robots also incorporated biomimetics, because they mimicked water strider insects. From reading articles I developed an understanding of what had been done with the robots to date and what had not. One disadvantage I noted was that the robots could not carry enough equipment to be useful and still had problems staying on the surface. Using information from studies done on actual water striders, I decided to attempt to evaluate the effects of trapping a thin layer of air within a nano-structure around a robot water strider's legs, because this was an evolved morphology of actual water striders which seemed to be of much benefit to them.

Eager to tryout some of my ideas but with a lab 8 hours away, I turned to mathematical modeling to help me understand the phenomena at play. My first attempt to understand the situation by oversimplifying the problem ended with a few graphs which were encouraging, but dead wrong. Every time I went back to the mathematical formulations, the problem became more and more complex and it ventured into math I had no experience with. Since my mentor was traveling and unavailable, it took my dad and myself weeks to correctly duplicate certain calculations much less create my own. Once I duplicated the calculations to determine the lift force of a water strider's leg, I then had to create my own equations to model what I was looking at. This took many attempts but I eventually ended up with something which made sense. The correct math ended up showing a much less drastic effect caused by the plastron (a thin layer of air surrounding actual water striders legs) than my initial calculations.

My experimental testing was done over two separate weeks at Carnegie Mellon. At the lab I had to design and carry out experiments which would provide meaningful data. There were graduate students in the lab who helped me with using lab equipment, and I had two or three meetings with my mentor, but my lab work was largely independent. After the first week, I was beginning to formulate a viable test but I flew home with no usable data, and feeling no further along on my project than when I left. The second week went much better, I was able to setup a viable experiment in the first two days and produce some good data through the remainder of the week.

All my ideas didn't really come together though until I set out to write my Intel paper. Once I got everything on paper I began the editing process. I spent hours reviewing editing notes and comments from my teachers and seeking out new opinions on my paper. I contacted another researcher in Canada to get another expert’s feedback. It was exhausting work, but when I read my paper before it was sent to Intel, my ideas made so much more sense to me than when I had began. I had streamlined the paper so far that I could not remove a sentence, each one said something critical. After Intel, I presented my research at many competitions, building comprehensive presentations from the solid base of my paper.

Many of my classmates, even good friends, say they didn't join the science research program because it was to much work, or they were not that interested in science. I no longer try to explain it to them, yeah it was a lot of work at times, but when you pursue something you are interested in it is a different type of work. I can't say it doesn't feel like work, because it did feel like work, but it's work with interior motivation. And after completing the project and working alongside so many others doing similar projects on such a wide scope of topics, not having an interest in science seems like it almost wouldn't be an issue. One younger student in the program decided to do his science research project on professional baseball! Also, even though you spend the entire time intensely studying one specific area of science, that is not what I feel was the most important thing I learned completing my project. My research experience has taught me a lot about the intersection of math, science, and writing, and it has reaffirmed my interest in engineering and critical problem solving. It taught me to work independently and has helped me developed valuable communication skills to ask for help when needed and has taken me from a timid presenter to a confident speaker. With student research, it is not about the significance of the research or about trying to learn about the topic, it is about growing as a scientist and a person.

1.0 Introduction:

Certain arthropods such as the water strider and the fisher spider have acquired the unique ability to walk on the surface of the water by exploiting the phenomenon of surface tension that occurs at the air-water interface. Water striders and other water-walking arthropods distribute their weight between supporting legs, creating dimples in the water's surface without penetrating it (Fig1.1). These dimples push against the weight of the water strider because the water is trying to return to its original state. Numerous studies have attempted to mimic the water strider's water walking abilities by creating robotic water striders with a similar morphological design. Despite our understanding of surface tension mechanisms, water striders are still far more adept at navigating along the free surface than their robotic counterparts, and it is clear that a deeper understanding is needed to produce robots on par with actual water striders. Such a robot would be exceptionally useful in monitoring marsh environments not suited for either floating or walking robots and would be much more easily converted into an amphibious robot because it already has the entire leg structure in place. Also, water strider robots could skate effortlessly over the surface of the water because they do not have to push water out of the way like a floating robot making it very fast and efficient.

Fig 1.1: A water strider on the water's surface. Note the dimples made by the supporting legs http://www.liv.ac.uk

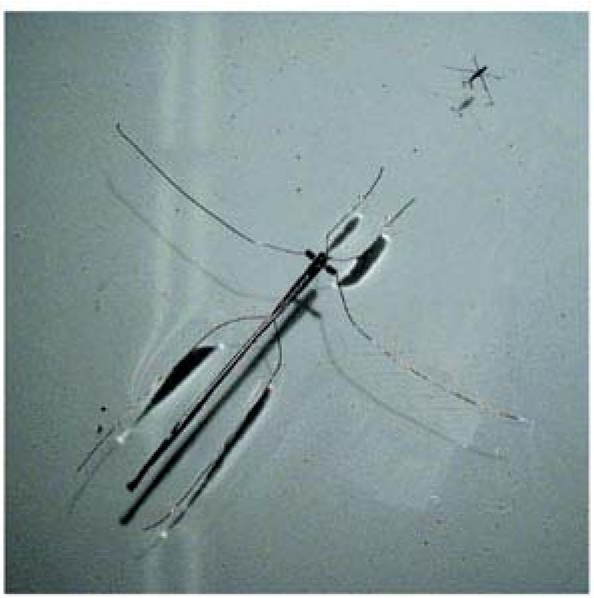

Fig 1.2: Robostrider, constructed by Hu et al. (2003), notice the real water strider in the upper right hand corner

In an early study, (Hu et al. 2003) a vortical structure was found in the wake of water striders that allows them to transfer momentum to the water. This finding was facilitated by the creation and testing of first water strider robot (Fig 1.2). Later studies have expanded this frontier, examining water striders' internal musculature (Takonobu et al., 2005), testing propulsive mechanisms and supporting the electronics needed by the robot (Song et al.,2007) (Fig 1.3). These prototype robots have yet to be deployed in actual environments because they are extremely limited in their capacity to bear loads required for functional missions. Current robots must carry at a minimum, a power supply and motors necessary to control the legs, however, even small surface disturbances in the water can cause them to break through and sink leaving the sensitive electronic equipment vulnerable to environmental damage. Furthermore, to be useful these robots need to bear additional devices including communications equipment, control computers and sensors to view and record the environment around them.

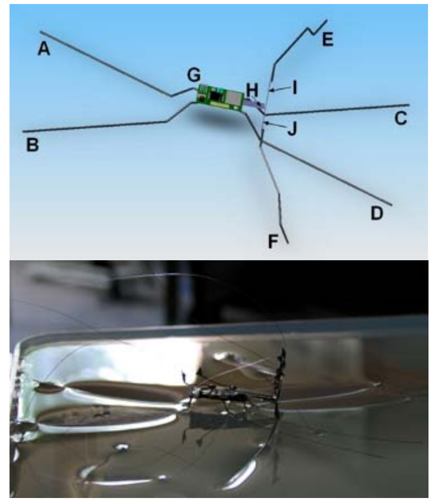

Fig 1. 3: A CAD rendering and picture of a water strider robot produced by Song et al.(2007)

Closer inspection of the insect's legs reveals unique physical characteristics that enable them to stay on the surface, despite frequent surface disturbances such as waves and heavy rain. Gao et al. (2004) noted that water striders have superhydrophobic legs which aide their ability to walk on the water's surface. Gao et al. (2004) concluded that this superhydrophobicity is achieved in two ways: (1) by excreting wax, water striders modify the chemical properties of their legs to increase the energetic cost of wetting, and (2) they have hierarchal nano-structures (Fig 1.4) that increase the surface area of their legs through surface roughening. Wenzel (1936) has shown that surface roughening, similar to the nano-structures used by water striders, increases the apparent contact angle between the leg and the water. *Contact angle* is a measure of the energetic cost of wetting of the material. Mathematical models of water strider legs in Song et al. (2007) have shown increases in contact angle can positively impact lift force. Gao (2004) determined that the hierarchical nano-structure on the water strider's legs is significantly more important to increasing the energetic cost of wetting than the wax. This superhydrophobic surface allows the water strider's leg to displace 300 times its own volume, allowing a single leg to support 15 times the body weight of the water strider. Artificial legs possessing the same properties as water strider legs are highly desired to advance the performance of water strider robotics and possibly allow them to jump on the water's surface as water striders can. Additionally, Gao (2004) noted that these hierarchical nano-structures (Fig 1.4) on the legs of water striders also trap a small cushion of air, known as a *plastron*. Gao (2004) found that actual water strider legs that created a plastron possessed almost eight times as much supportive potential as an un-textured synthetic leg with a similar contact angle.

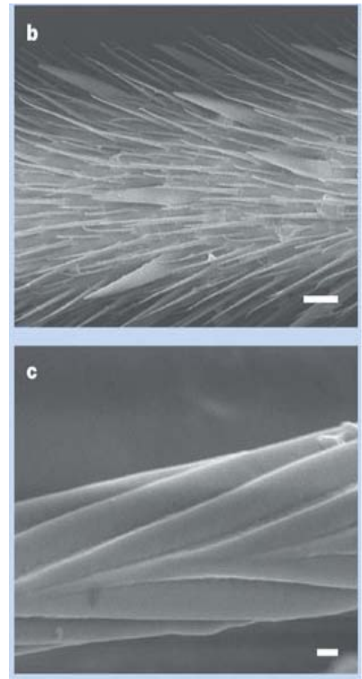

Fig 1.4: Scanning Electron Microscope image of the hierarchical structure of water striders nanohairs. TOP: the leg with numerous microsetae, BOTTOM: a single hair with nano scale groves. scale bars 20µm, 200nm. (Gao et al. 2004)

The plastron has been shown to have many benefits for certain species of arthropods which possess it. Most notably, it enables some species to perform plastron respiration to create breathable air under water (Shirtcliffe et. al, 2006). Shi et.al (2007) also concluded that the plastron greatly reduces the fluid drag on the water strider's legs, allowing them to move through the water with greater efficiency. However, the effects the plastron has on the lift force of water strider legs and how the apparent benefits of the plastron can be applied to current water strider robots remains to be thoroughly investigated.

Recently, in an attempt to mimic the hydrophobic properties of water strider's legs, low surface energy materials such as Teflon and Flurothane have been coated on robotic water strider legs (Song et al., 2007). These low surface energy materials increase the contact angle of the surface which makes it more resistant to wetting (hydrophobic). The application of these coatings helped to achieve hydrophobicity of the water strider robot legs, however this increase in contact angle was not found to produce a significant increase in lift force. Another recent study has attempted to increase the lift force of these robots by mimicking the surface roughening observed on the real insect's legs (Suzuki et al. 2007). Wires with etched metal surfaces were created, but again, little increase in lift force was achieved. Their study was the first to construct robotic water strider legs with nano-structures, however, its success was limited because the nano-structures constructed were not able to create a plastron similar to those observed by Gao(2004).

Previous research has attempted to mimic the lift force generated by water strider legs by altering the material and physical properties of the leg's surface, but it has largely ignored the potential of the plastron. It has been reported (Gao et al., 2004) that water striders use nano-hairs to generate plastrons to help them achieve greater lift forces. It is therefore an important next step to investigate the feasibility and advantages of using nano-hairs to create a plastron on the legs of water strider robots to increase lift force.

2.0 Purpose:

This research aimed to:

1. Model robotic water strider legs, based on their geometry, to determine if the supportive force provided by a plastron will provide a significant increase in the total lift force.
2. Determine design parameters for the fabrication of functional water strider legs displaying a plastron.

3. Construct various polymer samples to identify an ideal material and structure that is both superhydrophobic and capable of creating a plastron using nano-structures.
4. Test experimentally the fabricated samples to determine if the plastron can provide an increase in lift force.

3.0 Methods:

3.1 Phase 1: Mathematical model

The supportive force of the legs without nano-structures was solved mathematically based on the geometry of a cylinder (equations 1-7) (Suzuki et.al 2007). The vertical force per unit length (F) acting on the cylindrical model in Fig 3.1 was found by Suzuki et al. (2007) to consist of a buoyancy force (F_b) and a surface tension force(F_s).

$$F = F_b + F_s \tag{1}$$

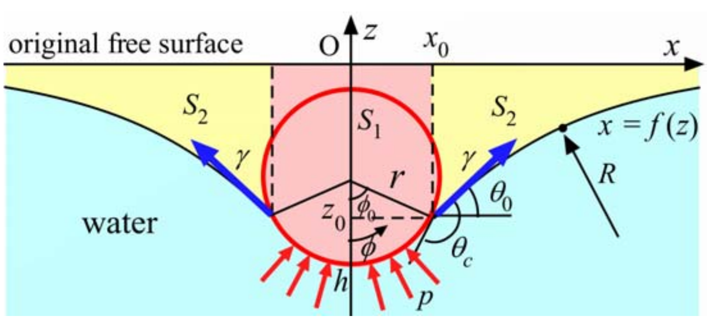

Fig 3.1: A 2D model of a wire supporting leg (Suzuki et.al, 2007)

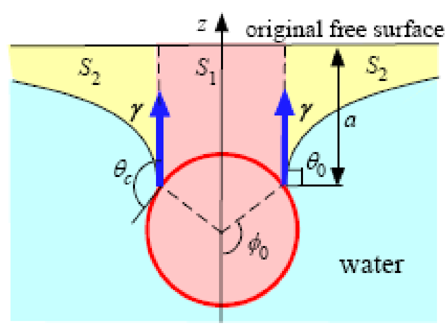

Fig 3.2: 2D model of a wire leg at maximum supportive force F_s=2γ (Suzuki et.al, 2007)

The buoyancy force, F_b was then determined by Suzuki et.al (2007) to be:

$$F_b = \rho g(-2 z_0 r \sin \phi_0 - r^2 \sin \phi_0 \cos \phi_0 + r^2 \phi_0) \tag{2}$$

And the surface tension force, F_s was determined to be:

$$F_s = 2\gamma \sin\theta_0 = \rho g S_2 \tag{3}$$

These forces are also proportional to the displaced water shown in red (F_b) and yellow (F_s) in Fig 3.1 and 3.2. In equations 2 and 3, φ_0 and θ_0 are related by:

$$\phi_0 = \pi + \theta_0 - \theta_c \tag{4}$$

The shape of the surface profile starting from the point (z_0, x_0) (the contact point of the water on the cylinder) was then defined as:

$$x = f(\mathrm{z}) = \frac{\mathrm{a}}{\sqrt{2}} \cosh^{-1}\left(\frac{\sqrt{2}a}{|z|}\right) - \sqrt{2a^2 - z^2} + C \tag{5}$$

$$f(0) = \infty, \quad f(\mathrm{z}_0) = x_0$$

Equation 5 has a constant, C, which is determined using the boundary conditions (Fig 3.2) where:

$$z_0 = -a = -\sqrt{\frac{2\gamma}{\rho g}} \tag{6}$$

And the slope of *f*(z) is:

$$f'(\mathrm{z}) = \frac{a^2 - z^2}{-z\sqrt{2a^2 - z^2}} \tag{7}$$

These equations can then be used to calculate the supportive force of the cylindrical leg.

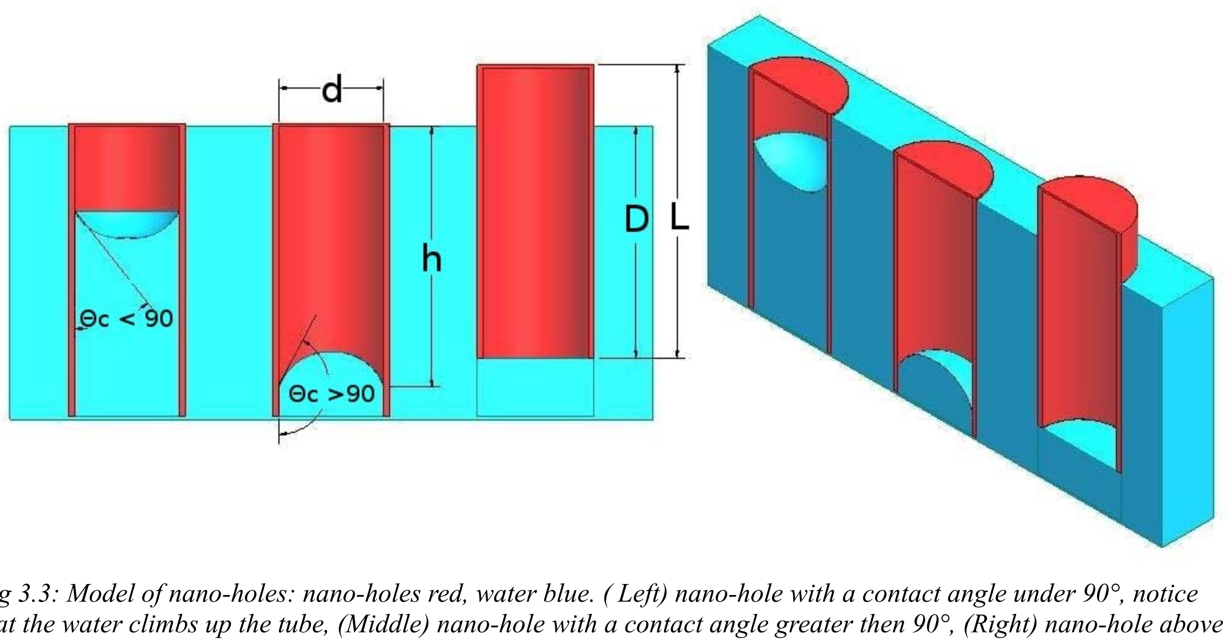

Fig 3.3: Model of nano-holes: nano-holes red, water blue. (Left) nano-hole with a contact angle under 90°, notice that the water climbs up the tube, (Middle) nano-hole with a contact angle greater then 90°, (Right) nano-hole above its critical depth

To calculate the impact of a leg with a plastron (represented here as a cylindrical leg with a layer of holes around it), we solved for the force produced by a single nano-sized hole based on its geometry (Fig 3.3). A nano-hole geometry was used for simplicity of modeling because it represents the basic principles of a plastron, but it eliminates the possibility of the air being pushed out between the hairs To quantify the forces involved, we first balanced the forces acting on the meniscus (water pressure, air pressure, and meniscus forces) to determine the size of the air pocket in the nano-hole. This was found to be:

$$0 = -P_{water} + P_{air} - P_{meniscus}$$

$$0 = -(P_1 + \rho g h) + \left(\frac{P_1 L}{(L - D + h)} \right) - \left(\frac{2\gamma Cos\,\theta}{r} \right) \tag{8}$$

When solved for h, the meniscus depth, this equation becomes:

$$h = \frac{P_1 + a(L-D) - \sqrt{(P_1 D + a(L-D))^2 - 4(-\rho g)\left(P_1 D - \frac{2\gamma Cos\,\theta}{r} \right)}}{2(-\rho g)} \tag{9}$$

The buoyancy and meniscus forces produced by the nano-hole were then solved based on the size of the air pocket determined from equation 9. In order to refer to the correct volume of air in different conditions, there are multiple buoyancy equations based on those conditions to be considered. The meniscus force equation was derived from the Young-Laplace equation for conditions where the meniscus was within or at the end of the hole.

If D≥L (submerged)

$$F_{bouancy} = (L - D + h)\rho g A$$

If h>L (end of hole)

$$F_{bouancy} = (L)\rho g A$$

If D≤L (Partially submerged)

$$F_{bouancy} = (h)\rho g A$$

If h>L (within hole)

$$F_{bouancy} = (D)\rho g A \tag{10}$$

$$F_{meniscus} = -\frac{2\lambda Cos\left(Cos^{-1}\left(\frac{D\rho gLr}{-2\lambda}\right)\right)}{r} \qquad (11)$$

Then by using equation 9, it is also possible to find when the meniscus will enter the tube by setting h=D and solving for D. This yields:

$$D_{critical} = \frac{-2\lambda Cos(\theta)}{\rho gLr} \qquad (12)$$

The force produced by a single nano-hole as given by the sum of equations 10 and 11 can then be multiplied by the number of holes on a given contact perimeter ($r_{contact}$) spaced at s_x diameters, and the number of holes on a given length spaced at s_y diameters to achieve the total force produced by the plastron on an entire leg. This formula can be superimposed onto Suzuki's (2007) model by setting $r_{contact}$ equal to φ_0 and using the same leg dimensions, however this situation does not account for the loss of the leg's mass due to the addition of air. Using our model, we investigated how the length, diameter and contact angle of the nano-holes affected the lift force they produced, and how the contact angle and the addition of a plastron affects the lift force of an entire leg.

$$F_{total} = \left(\frac{1}{s_x D} r_{contact} \Pi\right)\left(\frac{1}{s_y D} L\right) F_{perhole} \qquad (13)$$

3.2 Phase 2: Experimental Tests, Samples

Five different materials were employed to create 10 samples in an attempt to trap a plastron. Materials of varying thickness and with different arrangements of nano-structures were tested for the ideal physical characteristics necessary to achieve superhydrophobicity and maximize lift force. Most samples were polymers mixed and molded at the lab, the Teflon and Polypropylene filters were acquired from GE Water and Process Technologies (Minnetonka, MN, part #1215487, 1214237). Samples were cut into 4 identical circular disks with a diameter of 12.7mm using a custom circular punch. Samples were chosen based on their availability and physical properties. Materials tested and applicable geometries are listed in Table 3.1.

Table 3.1: Materials Tested and Applicable Geometries

Material	Thickness (mm)	Structure Shape	Structure Diameter (um)	Structure Height/Depth (um)	Structure Spacing (um)	Contact Angle
Polyurethane	.67	Mushroom Fibers	50, 100 (head)	100	120	110
Polyurethane	.61	Hairs	50	100	120	68
Polyurethane	.77	Flat	-	-	-	60
Pink Rubber	1.11	Holes	80	100	1:1	105
Pink Rubber	1.63	Holes	40	100	1:1	120
Pink Rubber	1.30	Flat	-	-	-	74
PDMS	1.09	Hairs	2			85
PDMS	1.20	Holes	200		400	112
PDMS	1.07	Flat	-	-	-	80
Polypropylene	.1	Filter	.1	-	-	130
Teflon	.14	Filter	.22	-	-	130

3.3 Contact Angles

To determine how the nano-structures affect the energetic cost of wetting of the samples, the contact angle was measured by placing a small drop of water on a flat sample and using a high resolution camera parallel to the flat surface to capture the image (Fig 3.4). The approximate contact angle was then measured directly from the image. The difference between the contact angles of each polymer sample with and without nano-structures was noted to demonstrate that the nano-hairs can cause a small increase in contact angles (Wenzel, 1936). The contact angle is important to the lift force measurements because it has been shown to directly affect the lift force of the leg.

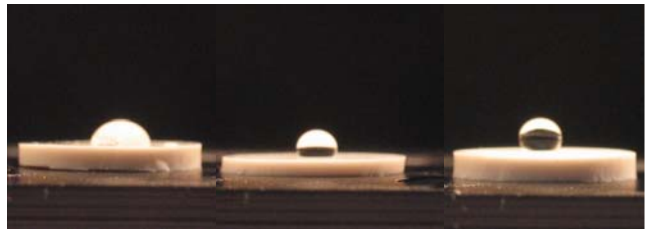

Fig 3.4: Contact angle images of three pink rubber samples, left to right, flat, big holes, small holes

3.4 Lift Force Testing

The lift force of samples was tested using a 50g load cell (Transducer Techniques, GSO-50), a motorized axis, and a custom computer program, used to control the motion stage and record the voltage returned by the load cell. A stage was designed to hold four flat 12.7mm in diameter samples and was leveled to ensure all feet came in contact with the surface of the water at exactly the same moment.

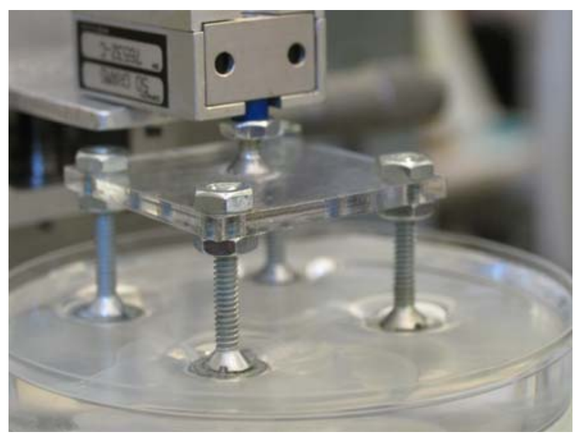

Fig 3.5: A trial in progress, a load cell measures how much the feet of the stage push back, The stage and load cell are moved by a motorized axis controller attached to the load cell.

Samples were suspended 15mm above the bottom of a dish of distilled water and the level of the water in the dish was monitored to ensure it remained constant. The sample and stage were then lowered at 0.2mm/s (Fig 3.5). The trial concluded when the load cell detected the stage making contact with the bottom of the dish. Following each trial, the stage was returned to the 15mm position and adequately dried prior to subsequent trials.

3.5 Analysis

The output files from the program were saved as text files (.txt) listing the trial run information and the data, consisting of 8 data points per millisecond. Each file contained the raw voltage from the load cell and the normalized voltage, which is the voltage difference from the start value. To analyze the load cell data, a load cell constant had to be determined from the load cell by placing known weights on the load cell and calculating the linear constant. The voltage from the load cell was converted into a force value by multiplying it by the determined constant.

To make the data files more useable, a program was written by this researcher in Visual Basic that imported the files into a spreadsheet program and manipulated the data. First, the time was normalized from the original computer timestamp so the beginning of the trial was set to zero. Then the normalized voltage was multiplied by the load cell constant. Finally, the data was reduced by a factor of eight to eliminate noise; this is done by averaging points together to yield one data point per millisecond and then writing the new values to a different spreadsheet for graphing.

4.0 Results

4.1 Modeling Results

In order to understand the effects of the plastron on a water strider leg, we first modeled an untextured water strider leg at various contact angles. Similar to the findings of Song (2007), it was found that lift force increases with contact angle; but as the contact angle increases, the benefit it provides lessens (Fig 4.1). This can be seen in the maximum values of Fig 4.1, the lift force of the 180° contact angle leg is clearly higher than the 40° leg; and as the contact angle increases, the difference between the maximums in the curve lessens.

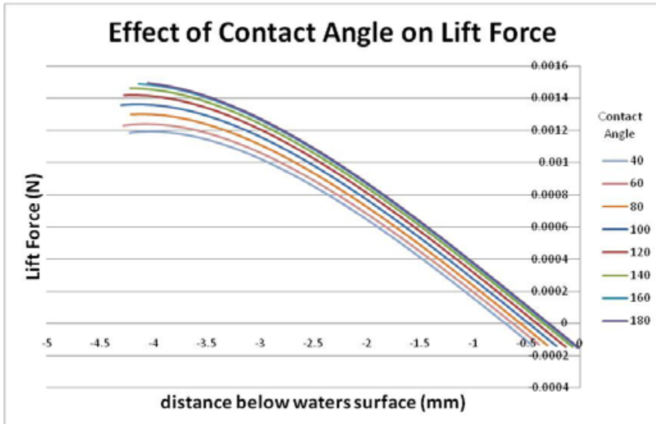

Fig 4.1: The lift force of a .5mm in diameter, 10 mm length of leg without a plastron at various contact angles. Height is distance below initial surface.

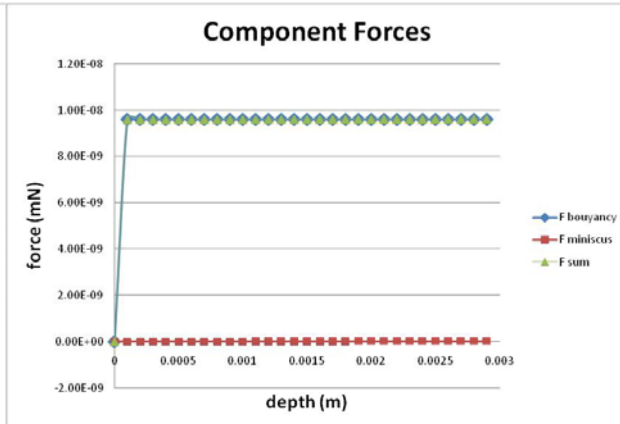

Fig 4.2: The component forces produced by a single nano-hole

We analyzed the forces produced by nano-holes by examining the component forces produced by a single nano-hole. As it can be seen in Fig 4.2, the supportive force of a nano-hole is primarily a result of the buoyancy of the air pocket, not the meniscus forces. This is shown by the meniscus forces (red curve) being nearly zero and therefore putting the sum curve (green) directly on top of the buoyancy (blue curve) because at any given depth, all the lift force comes from the buoyancy of the nano-hole.

Additionally, it was determined that the force produced by the nano-hole is independent of depth (Fig 4.3 B) except at 90°. Notice the red curve (90°) decreases with depth. This likely occurs

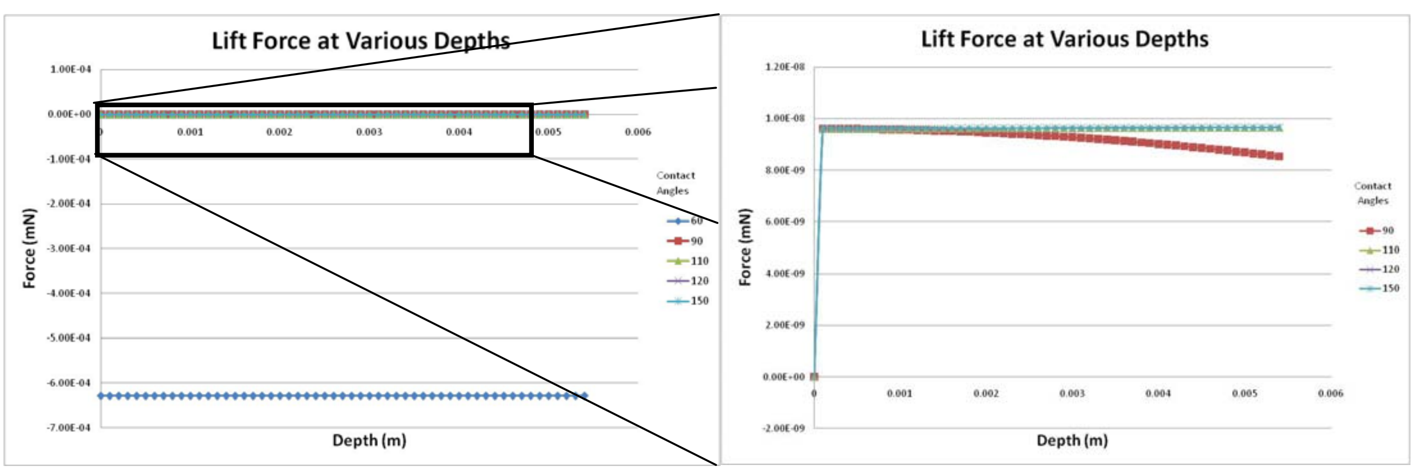

Fig 4.3: The forces produced by a single nano-hole at various depths, graph A (left) shows all the contact angles tested, graph B(right) is the same graph without the 60° contact angle graphed to show more detail.

because at 90° there are no meniscus forces to maintain the size of the air pocket as the leg is submerged so the buoyancy force steadily decreases; demonstrating the importance of the meniscus forces in this system. More importantly, Fig 4.3 B demonstrates the lift force's independence from contact angles greater than 90°. This can be seen most clearly in Fig 4.3 B where the lift force at 110° (green), 120°(purple) and 150°(light blue)are all the same. It is also notable that contact angles below 90° produce a negative lift force (notice the blue curve in Fig 4.3 A) because the meniscus not only pulls the tube down but also compresses the air, reducing the buoyancy force (Fig 4.3 A).

When examining how the length of the nano-holes affects the force provided by the plastron, a linear relationship was observed (Fig 4.4). This was expected, as the majority of the lift force is produced by the buoyancy force of the nano-hole, and the buoyancy of the hole would increase linearly with its volume. Hole diameter was also examined and it was found that even large holes of 0.1 mm in

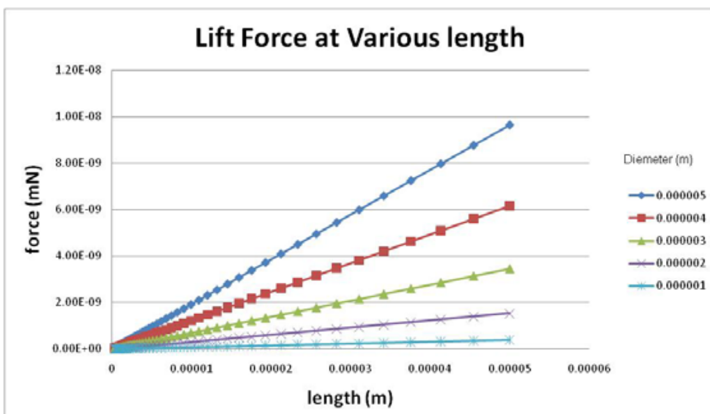

Fig 4.4: The forces produced by a single nano-hole as length increases

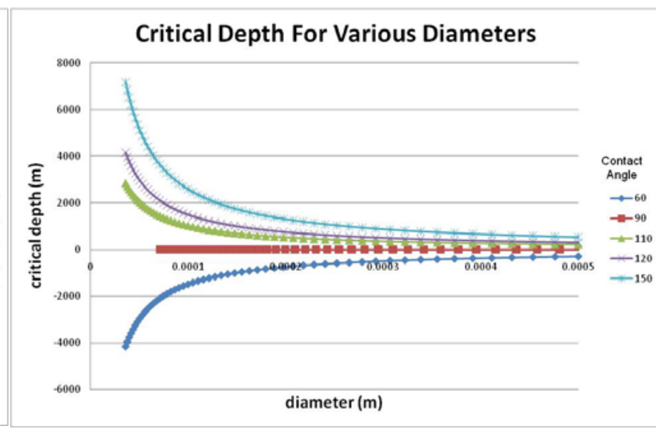

Fig 4.5: The critical depth change based on diameter

diameter with contact angles above 90° have extremely large critical depths (Fig 4.5), meaning it takes an incredible amount of force to overcome the resistance of the meniscus forces and compress the air. This suggests that for holes on the nano-scale, the meniscus will always be at the end of the nano-hole. Notice that as the holes get smaller (right to left) the critical depth quickly increases to over 1000m. This means that for an entire leg, the diameter of the holes does not affect the lift force as long as the total volume of air on the leg is the same. Therefore, two legs could achieve equal lift forces with many small holes or fewer large holes.

The modeling of the nano-holes showed that the majority of the lift force generated by a plastron is provided by the added displacement of the air, thus, adding holes as small as the ones modeled does not produce any useful increase in lift force. To evaluate the benefits of a larger plastron, Suzuki's (et al. 2007) model was expanded to include the negative lift provided by the density of steel, the material that makes up the leg, and the extreme case where the plastron is all air (no supporting structure). A 1mm diameter leg was modeled, however the actual diameter of the leg used in the calculation included the additional volume of a plastron (comprised of only air) that was a percent of the volume of the wire leg. Therefore a 500% plastron denotes a plastron 5 times the volume of the leg which causes the radius to increase about 2.5 times (Fig 4.6).

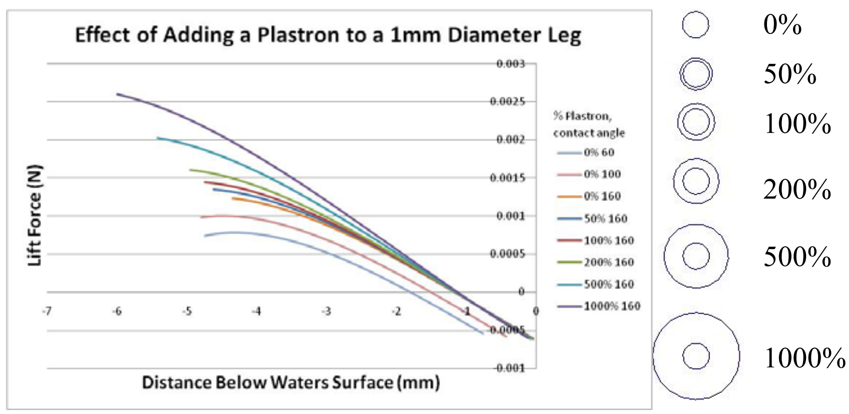

Fig 4.6: Lift force produced by a steel leg with a layer of air surrounding it. This volume of air is a given percent of the volume of the steel also represented by images on the right. The density of the steel was incorporated. Height is distance below initial surface.

We also assumed that the plastron should provide a contact angle around 160°. In this extreme case there is an evident benefit of the plastron (Fig 4.6). However, it requires a plastron nearly ten times the volume of the 1mm in diameter leg to double the force produced by the leg (with the same contact angle). When the initial size of the leg (without a plastron) decreases, the buoyancy becomes a smaller component of the total lift force and would require an even greater percentage plastron to double the lift force.

4.2 Lift Force Testing Results

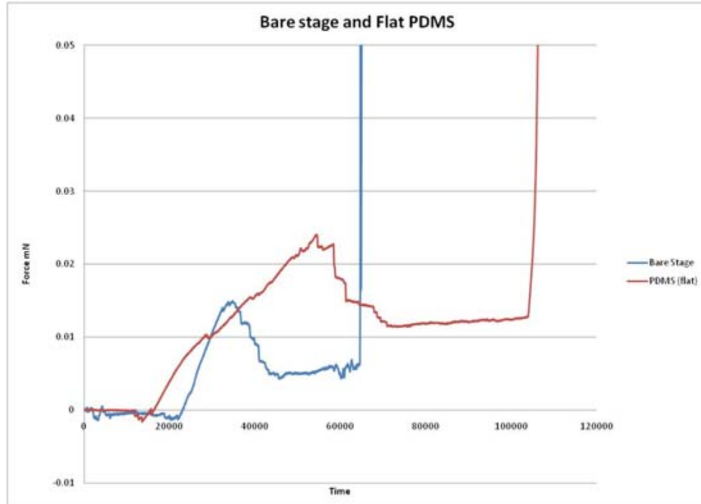

Fig 4.7: Lift force versus time for the bare testing apparatus and a flat PDMS sample (85 trials were conducted)

The output graphs (Fig 4.7) from trials show the time since the beginning of the trial and the lift force value. The lift force produced by a sample increased gradually until the sample began penetrating the surface, thereafter the buoyancy of the sample becomes the only measured component of the force (Fig 4.7).

It was found that adding any sample to the stage, even a very thin sample like Teflon, produced a fairly substantial increase in lift force. There was no observable benefit or detriment to having the nano-structures on the surface of the samples (Fig 4.8). Some differences in lift force can be accounted for by the differences in thicknesses of the samples, this can be confirmed by the evident change in the buoyancy values for the samples while the force provided by the meniscus does not change. The small volume of air trapped by the plastron of our samples does not seem to be able to produce enough force to be noticeable in the data. Also, the Teflon and Polypropylene graphs display deviant high trials for the samples. These deviant first trials were observed in all samples except the PDMS holes and flat pink sample. All these samples produced a higher lift force the first trial and the remainder of the trials were all consistent with each other. This suggests that the surface became wetted after the first trial despite the effort to dry the samples between trials, meaning that it no longer had any type of plastron, and its contact angle decreased, lowering the lift force.

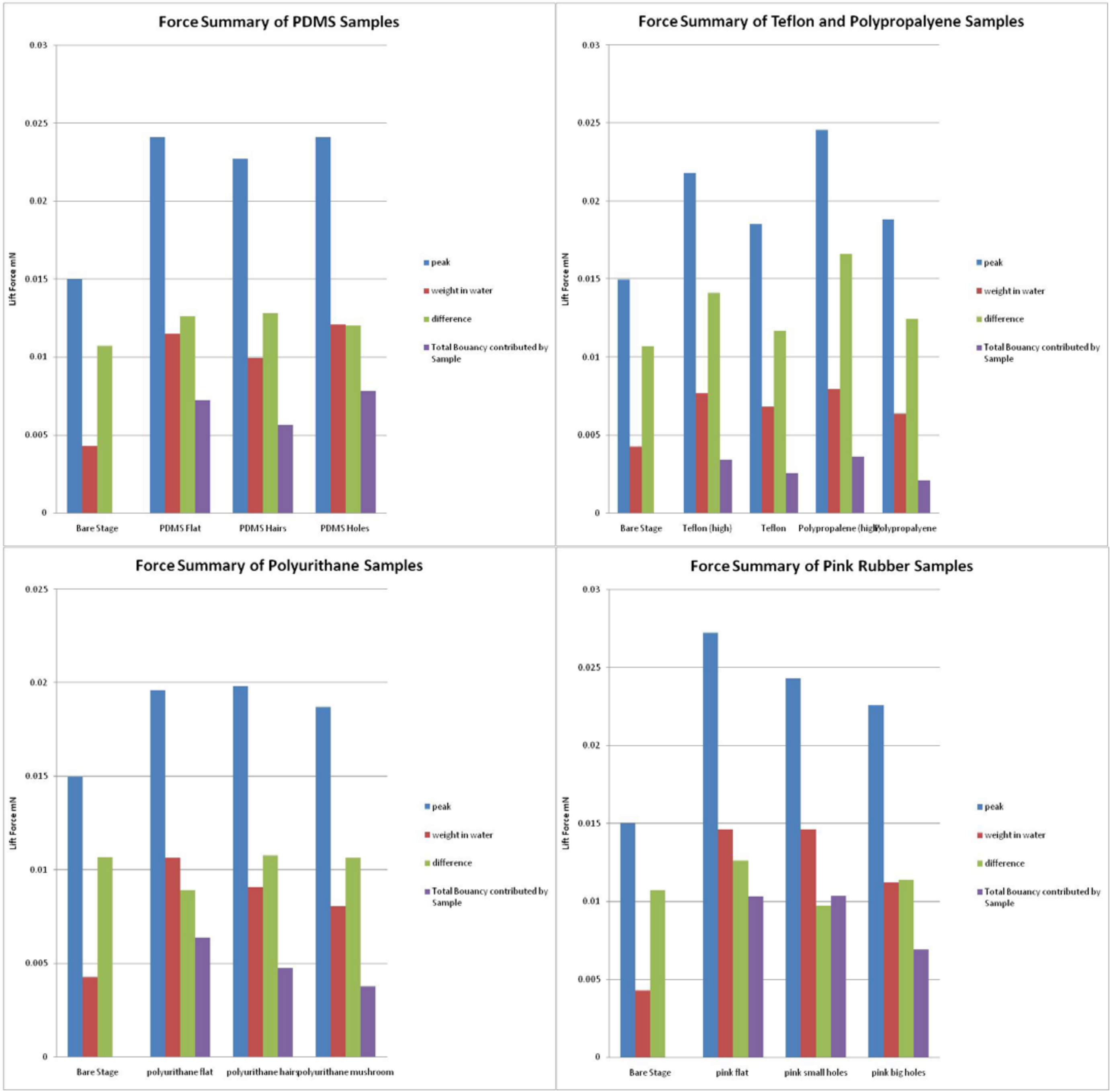

Fig 4.8: Force Summary for the four groups of sample, PDMS, Pink Rubber, Teflon/polypropylene filters, and Polyurethane. Bars show the peak lift force (high point in the graph), the buoyancy of the sample (the low after the peak), the difference between these two values, and the increase in buoyancy caused by the sample for a representative data set.

5.0 Discussion

This study is the first of its kind to examine the role the plastron plays in the lift force of a water strider leg. Mathematically it has been found that the plastron provides most of its additional lift force in the form of buoyancy forces produced solely by the displacement of water by the air trapped in the nano-structure. Our findings suggest that the plastron can provide an increase in lift force if it is sufficiently large, however none of the currently understood forces provided by a plastron or affected by the plastron can provide the increase observed by Gao et al.(2004) or Shi et al. (2007).

Even upon incorporating the relative densities of stainless steel and air, the buoyancy force produced by the plastron simply does not produce anything near the eight times increase found by Gao et al. (2004) when he tested actual water strider legs against manufactured legs without a plastron. Although our model assumes a simpler case than the experimental testing done by Gao et al. (2004), when we model legs on a similar scale it was found that as the diameter of a leg decreases, the lift force becomes predominantly composed of surface tension forces. Therefore, for legs as small as the ones used by Gao et al. (2004), an increase in contact angle and a slight increase in the displacement of the leg should not have any drastic effect on lift force. Although Gao's (et al. 2004) replica water strider leg may have been dissimilar to the actual water strider's leg in ways other than the contact angle and presence or absence of a plastron, it is doubtful that these minor differences could have caused an 8-fold difference in supportive force between the legs. Assuming that the contact angle and the presence/absence of a plastron were the only differences between these two legs, we failed to find any explanation for the difference in supportive force between the two legs. According to our data, no force provided by or affected by the plastron is capable of producing this difference.

Our experimental results supported our mathematical model in finding no significant increase in supportive force caused by the plastron, however our study was limited by the size, quality and even the questionable existence of plastrons created by the samples at hand. Our experimental results actually showed that after the first trial, nearly all samples became wetted and the lift force produced by them decreased. From our testing, it is evident that creating and maintaining a robust plastron is not easily realized. Design of a nano-structure as complex as those employed by the actual water strider insect is beyond the reach of current fabrication techniques. Future research should test other methods of nano-structure fabrication such as the self-assembled monolayers produced by electrochemical deposition and chemisorption techniques which were reported to create a visible plastron on a gold wire by Shi et al. (2007). The legs produced by Shi also showed a significant difference in supportive force between legs with a superhydrophobic plastron and flat gold wire legs (Fig 5.1).

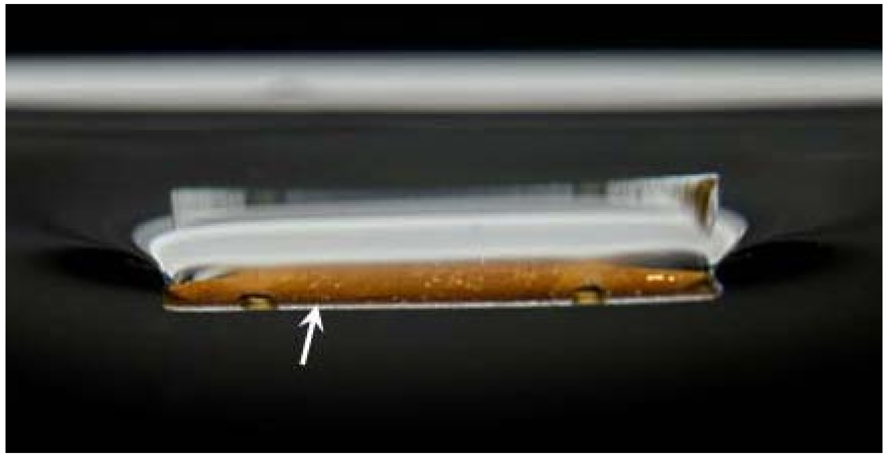

Fig 5.1: Visible plastron on a gold wire constructed by Shi (2007)

However he notes that the lift force returned to near zero after the leg penetrated the surface for both sample types. This would suggest almost no difference in the buoyancy of the legs. Shi et al. (2007) speculates that the additional buoyancy provided by the plastron may increase supportive force by altering the apparent density of the leg; but presents no quantifiable evidence for the difference and, it is evident that if only the buoyancy of the leg was being altered, the leg displaying a plastron would have a noticeably higher lift force when completely submerged (supported only by buoyancy).

While it may be that the contact angle also played a role in the increase found by Shi et al. (2007), other studies such as Song et al.(2007) have reported that increases in contact angle after the leg is hydrophobic does not increase lift force (Fig 5.2).

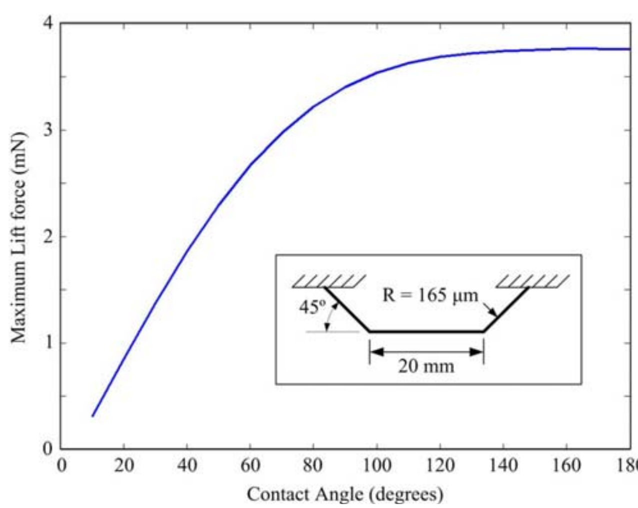

Fig 5.2: Modeling Results from Song (2007) showing that contact angle does not drastically affect lift force after 90°-100°

Suzuki et al. (2007) has also reported that surface texturing does not provide an increase in lift force either. Although the difference in supportive force found by Shi et al. (2007) was not as drastic as the one found by Gao et al. (2004), there is still a lack of understanding as to why this difference occurs.

The study herein furthers the current understanding of the mechanisms that water strider insects use to support their weight. Future studies should focus on modeling a plastron trapped by hairs to determine the most minimal structure required to trap an effective and maintainable plastron. Other polymers and geometries should be examined as they may provide a larger or more easily maintained plastron. We also suggest that current water strider robots could use hollow wire legs to test experimentally the effect of adding a certain amount of air to the system without using a plastron.

As our understanding of the plastron and the other mechanisms the water strider employs to support its weight increase, and we become able to replicate those abilities, we will be able to increase the load bearing capacity of water strider robots. As these robots can carry heavier loads, and as the electronics for these robots continue to get smaller and lighter, the applications for such small robots that can traverse the surface of fluids will continually expand.

6.0 Conclusion

Modeling results have shown that all currently understood forces provided by or affected by the plastron do not produce a drastic increase in the total lift force of a water strider robot leg. The forces are instead produced mainly as a result of buoyancy forces and are usually significantly smaller than the total force produced by the leg. Even the alteration of the contact angle caused by the plastron does not provide a significant increase in lift force.

The modeling results of this research do lead to a greater understanding of the plastron in general and what affects the overall performance of the plastron. This allows us to determine design parameters for fabrication of these nano-structures. The first and most important design parameter that must be met is that the contact angle of the material used to create the nano-structures must be greater than 90° as the meniscus forces produced by the large contact angle are necessary to maintain the air pocket. A contact angle of 90° would produce a steady decrease in force and contact angles less than 90° actually produce a negative force. It was also determined that the shape of the nano-holes does not affect the lift force, rather volume is the dependent variable because most of the force is contributed by buoyancy forces. The meniscus forces are still vitally important to maintaining the size of this air pocket, but they do not directly contribute to the lift force. Increasing the density of these nano-structures on the surface of the leg will also increase lift force as the volume of air trapped will increase.

When testing our experimental samples, no significant differences in supportive force were observed between textured and untextured samples. This agrees with our current model. Also, because the lift force of nearly all samples decreased after the first trial, we can assume that the surface became wetted. This leads us to question the existence of a plastron on the textured samples. We therefore conclude that further investigation of materials is needed to determine the optimal material and structure to trap a plastron.

7.0 Acknowledgements

I would like to thank my science research teachers Mr. Angelo Piccirillo and Miss Valerie Holmes for their insight and guidance on my project, and my parents for their support, especially of the extensive traveling my project entailed. I would also like to thank my mentor Dr. Metin Sitti for his assistance with my project and Mike Murphy and Onur Ozcan, for their assistance with lab equipment.

References

Crisp D.J, “The Stability of structures at a fluid interface,” *Trans. Faraday Soc.* 46:228-35, 1950.

Shi F., Niu J., Liu J., Liu F., Wang Z., Feng X., Zhang X. “*Towards UnderstandingWhy a Superhydrophobic Coating Is Needed by Water Striders,”* Advanced Materials vol 19, 2257-2261, 2007

Gao X, Jiang L,“*Water-repellent legs of water striders*,” *Nature,* vol 423, 4 November 2004.

Hu D. L., Chan B, Bush J. W.M, “The *Hydrodynamics of Water Strider Locomotion*,” *Nature,* vol 424, 7 August 2003.

Song Y.S, Sitti M, “ *STRIDE: A Highly Maneuverable and Non Tethered Water Strider Robot*,” *Robotics and Automation, 2007 IEEE International Conference on*, 10-14 April 2007.

Song Y.S, Sitti M, “Surface-*Tension-Driven Biologically Inspired Water Strider Robots: Theory and Experiments*,” *IEEE, Transactions On Robotics,* vol. 23, no.3, June 2007

Song Y.S, Suhr, Steve H, Sitti M, “*Modeling of the Supporting Legs for Designing Biomimetic Water Strider Robots”* Robotics and Automation, 2006. ICRA 2006. Proceedings 2006 IEEE International Conference on, 2006

Suter R.B, et. al.“*Locomotion On The Water Surface: Propulsive Mechanisms Of The Fisher Spider Dolomedes Triton”* The Journal of Experimental Biology 200, 2523-2538, 1997.

Suzuki K. et al. “*Water Strider Robots with Microfabricated Hydrophobic Legs*” Intelligent Robots and Systems 2007. 2007 IEEE/RSJ International conference on.

Takonobu H, et al., “*Water Strider's muscle arrangement-based robot”* Intelligent Robots and Systems 2005. (IROS 2005). 2005 IEEE/RSJ International conference on, pg 1754-1759, 2-6 August 2005.

Wenzel, “*Resistance of Solid Surfaces to Wetting By Water”* Industrial And Engineering Chemistry Vol 28, No. 6, 1936.